Indoxyl Sulfate Contributes to Selenium Deficiency and Renal Ferroptosis by Decreasing the Expression of Selenium Transport Protein Selenoprotein P

Takehiro Nakano,[1] Yutaka Kitazato,[1] Takumu Ogawa,[1] Kai Tokumaru,[2] Yuhi Shintani,[2] Takuma Yoshitake,[1] Kohei Yasuno,[1] Hitoshi Maeda,[1] Motoko Tanaka,[3] Kazutaka Matsushita,[3] Toru Maruyama,[1] and Hiroshi Watanabe[2]

Key Points

- Indoxyl sulfate (IS) is involved in the liver-kidney axis by inducing renal ferroptosis by selenium deficiency due to suppression of selenoprotein P (SEPP1) expression in the liver.
- IS concentrations were negatively associated with selenium concentrations and SEPP1 concentrations in serum from patients on dialysis.
- We propose the potential therapeutic strategy targeting the IS/SEPP1/glutathione peroxidase 4 pathway for CKD.

Abstract

Background The relationship between the progression of CKD and trace element deficiencies has attracted considerable attention. However, many aspects of trace element deficiency and the molecular mechanisms of CKD pathology remain unclear. In this study, we hypothesized that uremic toxins are involved in trace element deficiencies, which contribute to the progression of CKD.

Methods Adenine-induced CKD mice were used for *in vivo* study. Cultured hepatocytes were used for *in vitro* study.

Results Seventeen trace elements in plasma of CKD mice were measured using inductively coupled plasma mass spectrometry. Among these, selenium (Se) was identified as the trace element most significantly affected by the administration of oral spherical activated carbon (AST-120), an oral spherical activated carbon. CKD mice displayed reduced levels of Se in plasma, which was restored after the administration of AST-120. *In vivo* and *in vitro* experiments showed the uremic toxin indoxyl sulfate (IS) decreased expression of the Se transport protein selenoprotein P (SEPP1) in the liver. IS suppressed SEPP1 expression through increased production of reactive oxygen species by the organic anion transporting polypeptide/aryl hydrocarbon receptor/NADPH oxidase pathway. Increased reactive oxygen species led to the down-regulation of transcription factors for SEPP1, such as AMP-activated protein kinase/PGC-1α and microRNA-34a/HNF4α. Analysis of serum from patients on hemodialysis also suggested that IS is involved in reducing serum SEPP1 levels and exacerbating Se deficiency. Combination therapy with AST-120 and sodium selenite restored the supply of Se to the kidneys and increased glutathione peroxidase 4 expression, thereby exerting renoprotective effects by suppression of ferroptosis.

Conclusions This study highlights the key role IS plays in Se deficiency and renal ferroptosis by suppressing hepatic SEPP1 expression. The findings suggest potential therapeutic strategies that target IS and Se deficiency for the management of CKD.

Kidney360 6: 1448–1461, 2025. doi: https://doi.org/10.34067/KID.0000000837

Due to the number of contributing authors, the affiliations are listed at the end of this article.

Correspondence: Mr. Hiroshi Watanabe, email: hnabe@kumamoto-u.ac.jp

Received: February 17, 2025 **Accepted:** May 9, 2025
Published Online Ahead of Print: May 22, 2025

T.N. and H.W. contributed equally to this work.

See related editorial, "The Selenium Heist: Uremic Toxins Orchestrate Kidney Ferroptotic Stress in CKD," on pages 1427–1429.

Introduction

As renal function declines, the homeostasis of essential elements, including major and trace elements, becomes disrupted. Patients with CKD frequently develop abnormalities in mineral metabolism, such as hyperphosphatemia, hypocalcemia, and hyperkalemia, which are associated with cardiovascular complications.[1] Abnormalities in iron (Fe) metabolism leads to renal anemia.[2] It has become evident that patients with CKD are deficient in essential trace elements such as zinc (Zn), magnesium, and selenium (Se).[3] Indeed, deficiencies in these trace elements are reported to contribute to declines in renal function and the development of CKD-related complications.[4–8] Thus, controlling trace elements could be an important therapeutic strategy for CKD.

Several mechanisms underlying Zn and magnesium deficiencies have been reported, including (*1*) reduced intake due to loss of appetite and low-protein diets, (*2*) decreased absorption from the small intestine, (*3*) altered distribution caused by hypoalbuminemia, and (*4*) increased excretion by the kidneys.[9–14] For Fe metabolism, the uremic toxin indoxyl sulfate (IS) induces hepcidin production in the liver, which inhibits ferroportin. This, in turn, reduces both intestinal Fe absorption and Fe release from hepatocytes.[15] Although there is a close relationship between the progression of CKD pathology and some trace element deficiencies, several critical questions remain unanswered: (*1*) which trace elements fluctuate in CKD?; (*2*) what causes trace element fluctuations?; and (*3*) how is trace element deficiency involved in the exacerbation of CKD pathology?

It was hypothesized that increased plasma levels of uremic toxins in CKD affect trace element fluctuations. Initially, a comprehensive measurement of 17 trace elements in CKD mice was performed to clarify the molecular basis of trace element deficiencies associated with CKD pathology. Having identified trace elements that showed large fluctuations, we investigated the relationship between these fluctuations and uremic toxins. Finally, we evaluated a potential therapeutic strategy for CKD targeting uremic toxins and trace element deficiency using a CKD mouse model.

Methods

See Supplemental Methods and Supplemental Table 3 for detailed descriptions.

Animals

Institute of Cancer Research mice (male, 5 weeks old, Japan SLC, Shizuoka, Japan) were used. The animal care and use committee of Kumamoto University approved the protocols for all animal experiments (A2023-018).

Trace Element Concentration Measurements

Inductively coupled plasma mass spectrometry (Agilent 7900; Agilent Technologies, Santa Clara, CA) was used to measure trace element concentrations.

IS Concentration Measurements

High-pressure liquid chromatography (Extrema; Jasco Inc., Tokyo, Japan) was used to determine the concentration of IS in samples as described previously.[16]

Se Dynamics

Food intake, water consumption, feces, and urine output of mice were measured using a metabolic gauge (CL-0305/CL-0355; CLEA Japan, Inc., Tokyo, Japan) to determine the daily metabolic rate of Se.

In Vitro Experiments

HepG2 cells (RCB1886) were purchased from the RIKEN bioresource cell bank (Ibaraki, Japan). Primary cultured mouse hepatocytes were isolated from Institute of Cancer Research mice (male, 5 weeks old) using the collagenase perfusion method.[17]

Statistical Analyses

Experimental data are presented as mean±SEM. Statistical significance was assessed using Student's *t* test for comparisons between two groups. For data involving three or more groups, ANOVA followed by Tukey's multiple comparison test was performed. A P value of <0.05 was considered statistically significant.

Results

Effect of Oral Spherical Activated Carbon on Plasma Trace Element Variability in CKD Mice

In all, 17 trace elements in plasma of adenine-induced CKD mice were measured using inductively coupled plasma mass spectrometry. To evaluate the effect of uremic toxins on changes in plasma trace element concentration, oral charcoal absorbent (oral spherical activated carbon [AST-120]), which has a lowering effect on plasma uremic toxins, was administered to CKD mice (Figure 1A and Supplemental Table 1). Principal component analysis was performed to evaluate variation in the plasma levels of 17 trace elements. This analysis confirmed that levels of trace elements varied significantly in the CKD group compared with the control group (Figure 1B). Moreover, administration of AST-120 significantly altered levels of trace elements in the CKD group (Figure 1B). To determine which trace elements were most affected by AST-120 administration, volcano plots were generated for the CKD and CKD+AST-120 groups (Figure 1C). Of the 17 trace elements, Se displayed the greatest variation. The abnormally low plasma Se concentration in CKD mice significantly recovered after administration of AST-120 (Figure 1D).

Next, we evaluated whether the uremic toxin IS was involved in changes in plasma Se concentration induced by AST-120 administration. The plasma concentration of IS in CKD mice was significantly suppressed after administration of AST-120 (Figure 1E). In this case, plasma IS concentrations were negatively correlated with plasma Se concentrations ($R^2=0.854$; $P < 0.01$; Figure 1F). These findings suggested that IS may be involved in Se depletion in the pathogenesis of CKD.

Effect of AST-120 on a Plasma Se Transport Protein in CKD Mice

Selenoprotein P (SEPP1) is a Se-containing protein produced mainly in the liver that transports Se throughout the body.[18] Se deficiency occurs in humans with reduced SEPP1 expression[19] as well as in SEPP1 knockout mice.[20]

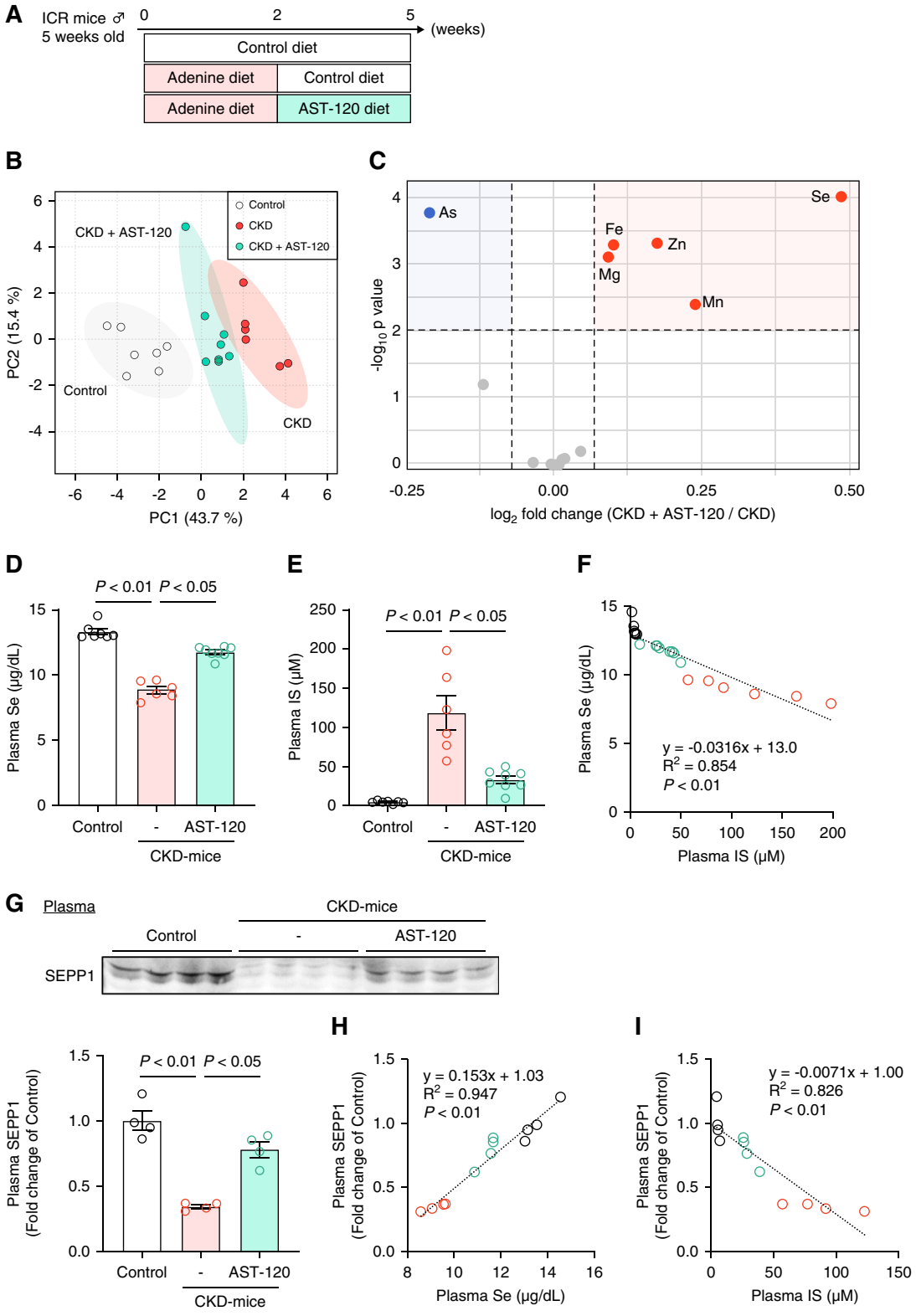

Figure 1. Effect of AST-120 on plasma trace element levels in CKD mice. (A) Experimental protocol for the effect of AST-120 on CKD mice. After randomization at 2 weeks after feeding a 0.2% adenine-containing diet, the AST-120 group was fed a diet containing 8% AST-120. (B) PCA score plot and (C) volcano plot of plasma trace element profiles in mice. The points indicate trace elements with content that reached a statistical difference according to the nonparametric test (log_{10} of the *P* value) and were altered by at least two-fold (log_2).

Figure 1. *Continued.* (D) Se and (E) IS concentrations in plasma. (F) Correlation between IS and Se concentrations in plasma. (G) SEPP1 protein level in plasma. Each 1 μg plasma sample was loaded. (H) Correlation between Se and SEPP1 protein level in plasma. (I) Correlation between IS and SEPP1 protein level in plasma. Data are expressed as mean±SEM (n=4). As, arsenic; AST-120, oral spherical activated carbon; Fe, iron; ICR, Institute of Cancer Research; IS, indoxyl sulfate; Mg, magnesium; Mn, manganese; PCA, principal component analysis; Se, selenium; SEPP1, selenoprotein P; Zn, zinc.

We hypothesized that IS contributes to plasma Se depletion by decreasing SEPP1 expression in CKD pathogenesis.

As shown in Figure 1G, plasma SEPP1 protein levels were lower in CKD mice in comparison with control mice, although the SEPP1 level recovered upon administration of AST-120. Moreover, plasma SEPP1 expression was positively correlated with plasma Se concentration (R^2=0.947; $P < 0.01$; Figure 1H). Furthermore, plasma IS concentrations were negatively correlated with plasma SEPP1 expression (R^2=0.826; $P < 0.01$; Figure 1I). These results suggest that IS could be involved in lowering plasma Se by decreasing SEPP1 expression.

Effect of AST-120 on Hepatic SEPP1 Expression in CKD Mice

Hepatic SEPP1 expression at the protein and mRNA level in CKD mice, which was lower than that in control mice, significantly recovered after administration of AST-120 (Figure 2, A and B). Hepatic IS content was increased in CKD mice but suppressed in AST-120–treated mice (Figure 2C). In this case, hepatic SEPP1 expression was negatively correlated with hepatic IS content (R^2=0.690; $P < 0.01$; Figure 2D), suggesting that IS contributes to Se deficiency by decreasing hepatic SEPP1 expression.

Similar studies were performed in other CKD model mice (5/6 nephrectomy [5/6Nx] model; Supplemental Figure 1A). Akin to adenine-induced CKD mice, decreased hepatic SEPP1 expression (protein and mRNA) and hepatic IS accumulation were observed in the 5/6Nx model (Supplemental Figure 1, B–D), in which hepatic IS content was negatively correlated with hepatic SEPP1 expression (R^2=0.711; $P < 0.01$; Supplemental Figure 1E). These observations suggest that IS also decreases hepatic SEPP1 expression in 5/6Nx model mice.

Effect of AST-120 on Se Dynamics in CKD Mice

Se from the diet is absorbed from the gastrointestinal tract[21] and undergoes primary metabolism in the liver to become incorporated into Se-containing proteins, such as SEPP1. Unwanted Se is excreted in urine as methylated metabolites.[22] In this study, we analyzed Se dynamics in CKD mice. No significant differences in Se intake or fecal Se excretion were observed among control mice and CKD mice with or without AST-120 (Figure 2, E and F). Urinary Se excretion was increased in CKD mice, but significantly suppressed by AST-120 administration (Figure 2G). Hepatic SEPP1 expression negatively correlated with urinary Se excretion (R^2=0.672; $P < 0.01$; Figure 2H). For the 5/6Nx model, no significant differences in Se intake or fecal Se excretion were observed (Supplemental Figure 1, F and G), although urinary Se excretion was increased (Supplemental Figure 1H). Hepatic SEPP1 expression also negatively correlated with urinary Se excretion (R^2=0.608; $P < 0.01$; Supplemental Figure 1I). These results indicate that AST-120 suppresses urinary excretion of Se by inhibiting IS-induced hepatic SEPP1 suppression.

Effect of AST-120 on Renal Se Content in CKD Mice

SEPP1 produced in the liver is reabsorbed from the luminal side of the renal tubules using megalin, located on the plasma membrane of tubular epithelial cells, to deliver Se to the kidney.[23] SEPP1 tubular reabsorption was reported to be reduced in megalin-mutant mice, resulting in decreased renal Se content.[24] In this study, we evaluated renal Se content in CKD mice. As shown in Figure 2I, renal Se content was decreased in CKD mice, but significantly recovered after AST-120 administration. Renal Se content positively correlated with hepatic SEPP1 expression (R^2=0.956; $P < 0.01$; Figure 2J), suggesting that IS is involved in Se depletion in the kidney by decreasing hepatic SEPP1 expression.

Effect of IS on SEPP1 Expression in Hepatocytes

Our data indicated that IS may have the ability to decrease hepatic SEPP1 expression. To clarify, HepG2 cells were incubated with IS and SEPP1 expression evaluated. As shown in Figure 3, A–D, SEPP1 expression was downregulated in a time- and concentration-dependent manner. Similarly, IS also decreased SEPP1 expression in primary cultured mouse hepatocytes (Figure 3, E and F). Therefore, IS directly decreases SEPP1 expression in hepatocytes. To confirm whether IS downregulates SEPP1 expression under Se supply, we evaluated SEPP1 expression (mRNA and protein) in HepG2 cells pretreated with sodium selenite[25] (100 nM). As shown in Figure 3, G and H, the increase in SEPP1 protein and mRNA expression by sodium selenite was suppressed by IS. These results indicate that IS decreases SEPP1 expression in hepatocytes even under Se supply.

Next, we compared the effects of seven albumin-binding uremic toxins (IS, *p*-cresyl sulfate, phenyl sulfate, hippuric acid, indole acetic acid, kynurenic acid, and 3-carboxy-4-methyl-5-propyl-2-furanpropanoic acid) on SEPP1 expression in HepG2 cells. The sharpest decrease in SEPP1 expression was observed in the presence of IS (Figure 3, I and J).

Molecular Mechanism of IS-Induced Decrease in SEPP1 Expression

HepG2 cells were used to elucidate the molecular mechanism of the IS-induced decrease in SEPP1 expression. Hepatocytes take up IS into the cell using an organic anion-transporting polypeptide (OATP). First, we evaluated the effect of IS on SEPP1 expression in HepG2 cells pretreated with three OATP inhibitors (probenecid, estrone sulfate, and rifampicin), according to a previous report.[26] As shown in Supplemental Figure 2A, the decrease in SEPP1 expression after addition of IS was

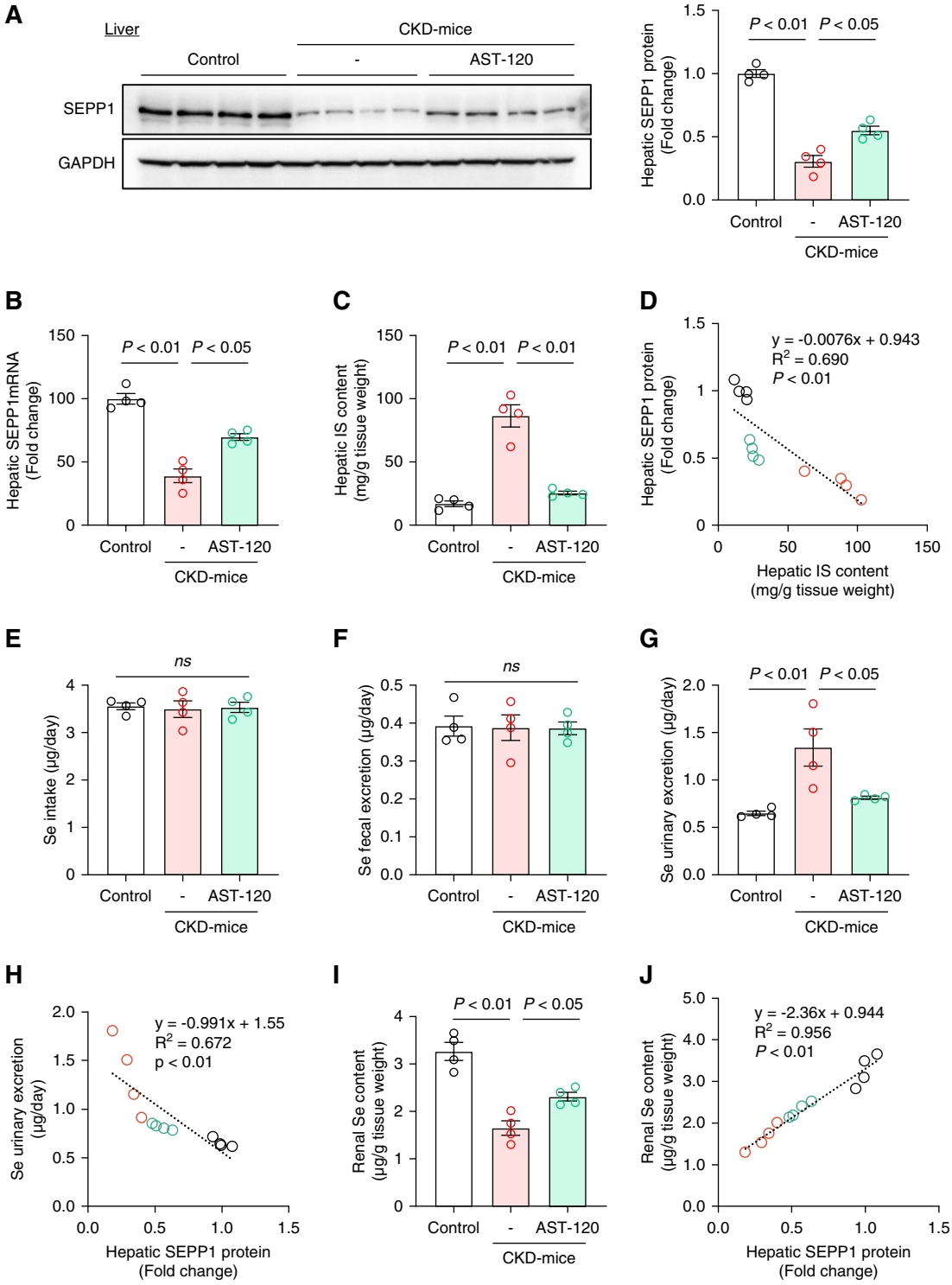

Figure 2. Effect of AST-120 on hepatic SEPP1 expression and renal Se content in CKD mice. Expression of SEPP1 (A) protein and (B) mRNA in the liver. (C) IS content in the liver. (D) Correlation between IS content and SEPP1 protein expression in the liver. (E) Daily Se intake levels. (F) Daily Se fecal excretion levels. (G) Daily Se urinary excretion levels. (H) Correlation between SEPP1 protein expression in the liver and daily Se urinary excretion levels. (I) Se content in the kidney. (J) Correlation between SEPP1 protein expression in the liver and Se content in the kidney. Data are expressed as mean±SEM (n=6–8).

suppressed in the presence of these OATP inhibitors. The IS-induced decrease in SEPP1 expression was significantly suppressed in the presence of an OATP inhibitor (probenecid), aryl hydrocarbon receptor (AhR) inhibitor (2-methyl-2H-pyrazole-3-carboxylic acid (2-methyl-4-o-tolylazo-phenyl)-amide-223191), NADPH oxidase inhibitor

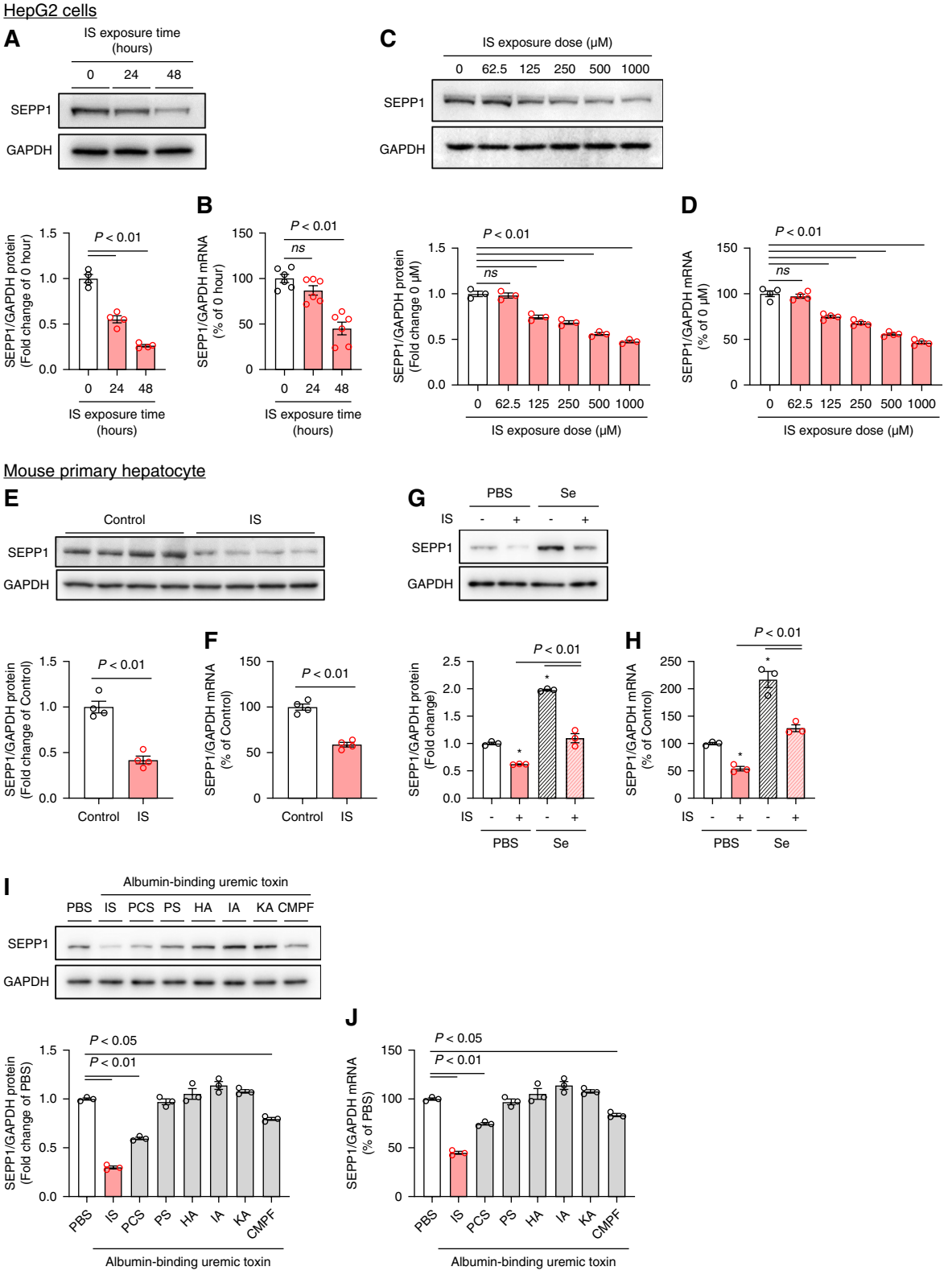

Figure 3. Effect of IS on hepatic SEPP1 expression. Time-dependent effects (0, 24, and 48 hours) of IS (1 mM) on the expression of SEPP1 protein (A) and (B) mRNA in HepG2 cells. Dose-dependent effects (0–1 mM) of IS on the expression of SEPP1 protein (C) and (D) mRNA in HepG2 cells for 48 hours. Effect of IS (1 mM) on SEPP1 protein (E) and (F) mRNA expression in mouse primary hepatocytes for 24 hours. Effect of IS (1 mM) and sodium selenite (100 nM) on SEPP1 protein (G) and (H) mRNA expression in HepG2 cells for 48 hours. Effect of

Figure 3. *Continued.* seven albumin-binding uremic toxins (IS, PCS, PS, HA, IA, KA, CMPF: 1 mM) on SEPP1 protein (I) and (J) mRNA expression in HepG2 cells for 48 hours. *$P < 0.05$ compared with IS (−) in the absence of sodium selenite. Data are expressed as mean±SEM (n=3–6). CMPF, carboxy-4-methyl-5-propyl-2-furanpropanoic; HA, hippuric acid; IA, indole acetic acid; KA, kynurenic acid; PCS, *p*-cresyl sulfate; PS, phenyl sulfate.

(diphenylene iodonium), antioxidant (ascorbic acid [AsA]), and mitochondrial reactive oxygen species (ROS) scavenger (mitochondria-targeted antioxidant compound piperidine nitroxide [2,2,6,6-tetramethylpiperidin-1-oxyl]; Figure 4A). These results suggest that after IS enters the cell using OATP, there is a decrease in SEPP1 expression through production of ROS (including mitochondrial ROS) upon activation of NADPH oxidase by AhR signaling. In HepG2 cells, SEPP1 expression was also decreased when hydrogen peroxide, an ROS inducer, was added, and suppressed in the presence of an antioxidant (AsA; Figure 4B). Among the seven albumin-bound uremic toxins, only IS was found to significantly produce ROS (Figure 4C). These results demonstrate that induction of ROS is important for IS-induced SEPP1 suppression.

Transcription factors sterol regulatory element binding protein 1c, PGC-1α, and HNF4α bind to the promoter region of SEPP1 and regulate SEPP1 transcription.[27,28] Thus, IS may downregulate SEPP1 by altering the expression of these transcription factors. IS had no effect on sterol regulatory element binding protein 1c mRNA expression but significantly decreased PGC-1α and HNF4α expression (Supplemental Figure 2, B–D). IS decreases PGC-1α expression in myocytes[29] and dephosphorylates AMP-activated protein kinase (AMPK) (upstream of PGC-1α) in cardiomyocytes.[30] We found IS also decreased AMPK phosphorylation and PGC-1α protein expression in HepG2 cells, and these changes were suppressed in the presence of an antioxidant (AsA) or AMPK activator (Figure 4D). Moreover, IS-induced SEPP1 suppression was recovered by the presence of the AMPK activator (Figure 4E). These results indicate IS-derived ROS downregulates SEPP1 expression by dephosphorylating AMPK and decreasing PGC-1α expression (ROS↑/phospho-AMPK↓/PGC-1α↓/SEPP1↓).

IS is also reported to increase microRNA-34a-5p (miR-34a-5p) expression in vascular endothelial cells,[31] and miR-34a-5p decreased HNF4α in hepatocytes.[32] Here, IS increased miR-34a-5p expression and decreased HNF4α expression, and these changes were suppressed by AsA or an miR-34a-5p inhibitor (Figure 4, F and G). Furthermore, IS-induced SEPP1 suppression recovered in the presence of an miR-34a-5p inhibitor (Figure 4H). These results indicate that IS-derived ROS decreased SEPP1 expression by increasing miR-34a-5p expression and decreasing HNF4α expression (ROS↑/miR-34a-5p↑/HNF4α↓/SEPP1↓). Thus, IS increases ROS production through the OATP/AhR/NADPH oxidase pathway and decreases SEPP1 expression by modulating the AMPK/PGC-1α and miR-34a-5p/HNF4α pathways (Figure 4I).

Relationship between Serum Se and IS Concentrations in Patients on Dialysis

Next, we investigated the relationship between serum Se and IS concentrations in patients on dialysis. A total of 55 patients on hemodialysis (33 male and 22 female patients) were enrolled in this study. All blood samples were collected before dialysis. The molecular weight of SEPP1 is 43.2 kDa, which means SEPP1 is not easily removed by dialysis. Our findings showed that serum IS concentrations negatively correlated with serum Se concentrations (R^2=0.824; $P < 0.01$; Supplemental Figure 3A). Furthermore, among patients on dialysis, those with high serum IS (>100 μM) and low serum Se (<10.5 μg/dl) concentrations had lower serum SEPP1 expression compared with those with low serum IS and normal serum Se concentrations (cutoff value for IS: 100 μM; normal value for Se[33]: 10.5–17.3 μg/dl; Supplemental Figure 3B). Interestingly, age of the patients on dialysis was negatively correlated with serum Se concentration (overall: R^2=0.322; $P < 0.05$, male: R^2=0.322; $P < 0.05$, female: R^2=0.246; $P < 0.05$), although serum IS concentration was a more important factor (Supplemental Figure 3C). The results of this observational study indicate that IS could be involved in the decrease in serum SEPP1 levels and Se deficiency in patients on hemodialysis.

Inhibition of Renal Ferroptosis By Therapeutic Intervention Targeting IS/SEPP1/Glutathione Peroxidase 4 Pathway in CKD Mice

Administration of AST-120 alone did not fully restore renal Se content in CKD mice (Figure 2I). It is assumed that Se delivered to the kidney as SEPP1 is resynthesized into functional Se-containing proteins (*e.g.*, glutathione peroxidase 4 [GPX4]).[34] GPX4 regulates intracellular redox balance by reducing lipid peroxides in cell membranes to alcohols using reduced GSH as a cofactor, thereby lessening the accumulation of lipid peroxide. Indeed, GPX4 knockout mice developed AKI with renal tubular ferroptosis, suggesting that GPX4 is deeply involved in the redox balance of the renal tubules.[35] We hypothesized that treatment of CKD using Se supplementation alongside AST-120 would increase SEPP1 production in the liver, resulting in enhanced renoprotection. The therapeutic effects of (*1*) AST-120, (*2*) intraperitoneal sodium selenite, and (*3*) a combination of AST-120 and sodium selenite on adenine-induced CKD in mice were compared (Figure 5A). A combination of AST-120 and Se supplementation (Figure 5, B–D) upregulated hepatic SEPP1 expression, and plasma SEPP1 levels were restored to normal. In addition, the decrease in Se content in plasma and kidney of CKD mice largely recovered after combination treatment (Figure 5, E and F). Furthermore, decreased expression of GPX4 in renal tissues of CKD mice was restored after combination therapy, which positively correlated with renal Se content (R^2=0.825; $P < 0.01$; Figure 5, G and H). These results indicate that combined treatment of AST-120 and Se supplementation for CKD promotes Se supply to the kidneys by SEPP1, resulting in restoration of GPX4 expression.

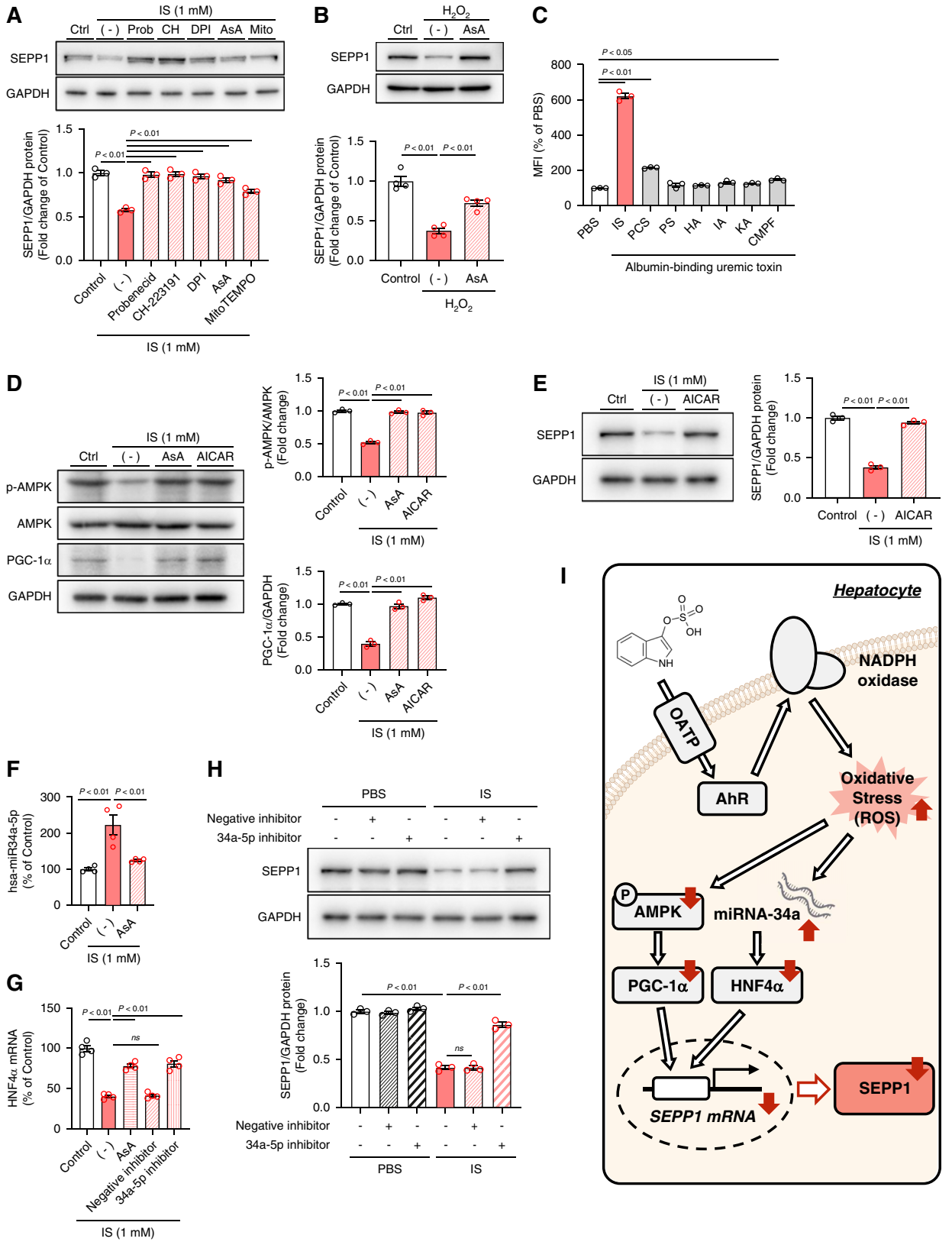

Figure 4. Molecular mechanism of IS-induced SEPP1 suppression. (A) Effect of an OATP inhibitor (probenecid [0.5 mM]), AhR inhibitor (CH-223191 [10 μM]), NADPH oxidase inhibitor (DPI [10 μM]), antioxidant (AsA [0.5 mM]), and MitoTEMPO (10 μM) on IS (1 mM)-induced SEPP1 suppression in HepG2 cells. Cells were exposed to each inhibitor for 1 hour and then incubated with IS for 48 hours. (B) Effect of the oxidant (H_2O_2 [100 μM]) and antioxidant (AsA [0.5 mM]) on SEPP1 protein expression in HepG2 cells. Cells were exposed to AsA for 1 hour and then incubated with H_2O_2 for 48 hours. (C) Effect of seven albumin-binding uremic toxins (IS, PCS. PS, HA, IA, KA,

Figure 4. *Continued.* CMPF: 1 mM) on the production of ROS in HepG2 cells for 1 hour. (D) AMPK activity (p-AMPK/AMPK) and PGC-1α protein expression in HepG2 cells were detected. Cells were treated with AsA (0.5 mM) or AICAR (0.5 mM) for 1 hour and then incubated with IS (1 mM) for 48 hours. (E) Effect of AICAR (0.5 mM) on IS (1 mM)-induced SEPP1 suppression in HepG2 cells. Cells were exposed to AICAR for 1 hour and then incubated with IS for 48 hours. (F) miR34a-5p expression in HepG2 cells was determined. Cells were treated with AsA (0.5 mM) for 1 hour and then incubated with IS (1 mM) for 48 hours. (G) Effect of the miR34a-5p inhibitor (20 nM), miRNA-negative inhibitor (20 nM), and AsA (0.5 mM) on IS (1 mM)-induced HNF4α mRNA suppression in HepG2 cells. Cells were exposed to each inhibitor for 1 hour and then incubated with IS for 48 hours. (H) Effect of the miR34a-5p inhibitor and miRNA-negative inhibitor on IS (1 mM)-induced SEPP1 suppression in HepG2 cells. Cells were exposed to each inhibitor for 1 hour and then incubated with IS (1 mM) for 48 hours. (I) Schematic showing the molecular mechanism of IS-induced SEPP1 suppression. Data are expressed as mean±SEM (n=3–4). AhR, aryl hydrocarbon receptor; AICAR, AMPK activator; AMPK, AMP-activated protein kinase; AsA, ascorbic acid; CH, 2-methyl-2H-pyrazole-3-carboxylic acid (2-methyl-4-o-tolylazo-phenyl)-amide; DPI, diphenylene iodonium; miRNA, microRNA; MitoTEMPO, Mitochondria-targeted antioxidant compound piperidine nitroxide (2,2,6,6-tetramethylpiperidin-1-oxyl); OATP, organic anion transporting polypeptide; p-AMPK, phospho-AMPK; ROS, reactive oxygen species.

Finally, we evaluated the renoprotective effects of AST-120 and sodium selenite combination treatment on CKD mice. Decreased renal function (increased BUN, serum creatinine, urine volume, and urinary protein and decreased creatinine clearance) in CKD mice was significantly suppressed by combination treatment as compared with AST-120 or sodium selenite alone (Supplemental Figure 4, A–E). In addition, increased expression of a marker of tubular damage (kidney injury molecule-1 mRNA) in CKD mice was also significantly suppressed after combination treatment (Supplemental Figure 4F). Increase of IS in plasma and kidney of CKD mice was also markedly suppressed by the combination treatment (Supplemental Figure 4, G and H). Renal histological analysis (periodic acid–Schiff staining) identified abnormal tubules in the renal cortical region of CKD mice. However, this tissue damage was suppressed by the combination treatment (Figure 6, A and B). Moreover, the combination treatment significantly reduced the number of TUNEL-positive cells (Figure 6, A and C). Enzyme immunostaining for 4-hydroxynonenal was performed to evaluate the accumulation of lipid peroxides, a marker for ferroptosis. The accumulation of lipid peroxides (brown) observed in CKD mice was markedly suppressed by the combination treatment (Figure 6, A and D). Next, we measured the level of lipid peroxide (malondialdehyde) in renal tissues. The increase in malondialdehyde in CKD mice was suppressed after combination treatment (Figure 6E). Furthermore, the combination treatment reduced the elevated plasma albumin oxidation levels, a marker of systemic oxidative stress, in CKD mice (Figure 6F). Renal expression of a ferroptosis marker (hyperoxidized PRDX3) was elevated in CKD mice but significantly decreased after combination treatment (Figure 6G). On the basis of these results, we found that the combination treatment of AST-120 and Se supplementation exerted a renoprotective effect through inhibition of ferroptosis. The mechanism may involve restoration of Se supply to the kidneys resulting in recovery of GPX4 expression and a consequent decrease in lipid peroxide, a ferroptosis-inducing factor (Figure 6H).

Discussion

Recently, the relationship between progression of CKD and onset of its complications with trace element deficiency has attracted attention.[3] However, aspects of fluctuations in trace elements and their molecular mechanisms in CKD pathology remain unclear. To clarify the molecular basis of trace element deficiencies associated with CKD, we investigated the corresponding relationship with uremic toxin accumulation.

We comprehensively measured 17 trace elements in plasma of CKD mice. Among these, Se was identified as the trace element most significantly affected by AST-120 administration. Indeed, AST-120 administration restored the low levels of plasma Se found in CKD mice to normal levels. Furthermore, IS decreased the expression of the Se transport protein SEPP1 in the liver. In addition, using HepG2 cells, we demonstrated that IS suppresses SEPP1 expression through increased ROS production through the OATP/AhR/NADPH oxidase pathway. Increased ROS leads to inhibition of transcription factors, such as AMPK/PGC-1α and microRNA-34a (miR-34a)/HNF4α. Moreover, studies using serum from patients on hemodialysis also suggested that IS could contribute to reduced serum SEPP1 levels and Se deficiency. Thus, we performed a combination therapy using AST-120 and sodium selenite. This combination therapy restored Se supply to the kidneys and increased GPX4 expression by SEPP1, thereby exerting renoprotective effects by suppression of ferroptosis.

Trace element deficiencies have been reported in both nondialysis patients with CKD and patients on hemodialysis. Deficiencies in Fe, Zn, and Se were commonly observed.[3,36–38] In CKD mice, we also found that plasma concentrations of Fe, Zn, and Se were significantly reduced (Supplemental Table 2). Furthermore, the plasma concentrations of these trace elements in CKD mice were within the range observed in human deficiency states, supporting the usefulness of this CKD mice model for evaluating trace element deficiencies in CKD.

We demonstrated that IS contributes to Se deficiency by reducing SEPP1 expression. Dietary Se is incorporated into Se-containing proteins, such as SEPP1, enabling its retention in the body.[21] Se that is not retained is rapidly excreted in urine.[22] Therefore, when SEPP1 expression is downregulated, the ability of the body to retain Se is diminished. Indeed, increased urinary Se excretion observed in CKD mice was suppressed after AST-120 administration, and hepatic SEPP1 expression showed a negative correlation with urinary Se excretion (Figure 2H). These data suggest SEPP1 expression is an indicator of the capacity of the body to retain Se. Renal Se content of CKD mice was not fully

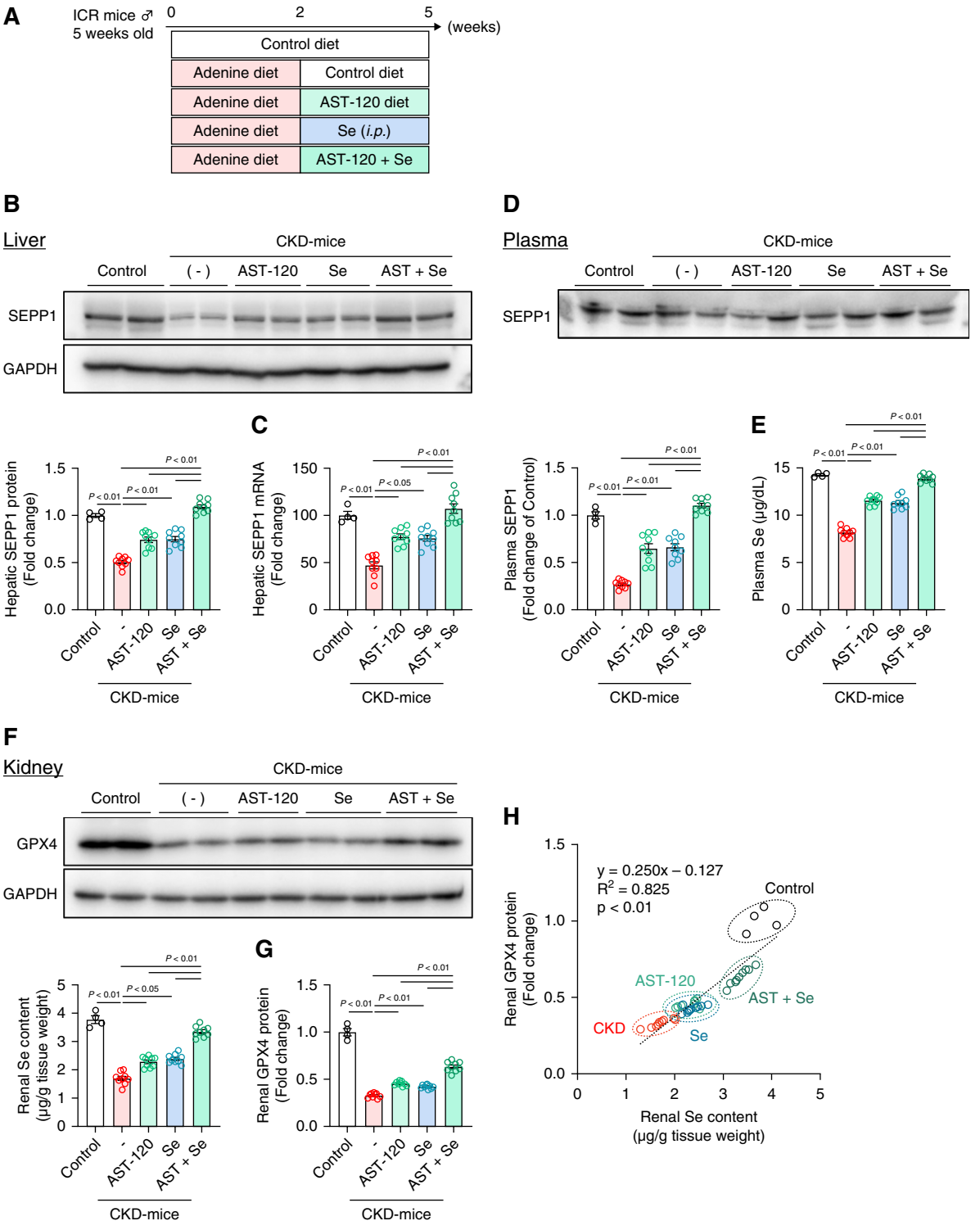

Figure 5. Therapeutic intervention targeting the IS/SEPP1 pathway in CKD mice. (A) Experimental protocol for the effect of AST-120 and Se supplementation on CKD mice. After randomization at 2 weeks after feeding 0.2% adenine-containing diet, the AST-120 group was fed a diet containing 8% AST-120 and the Se supplementation group received sodium selenite (0.5 μg/g BW intraperitoneally, daily). Expression of SEPP1 (B) protein and (C) mRNA in the liver. (D) SEPP1 protein and (E) Se levels in plasma. (F) Se content and (G) GPX4 protein expression in the kidney. (H) Correlation between Se content and GPX4 protein expression in the kidney. Data are expressed as mean±SEM (n=4–9). GPX4, glutathione peroxidase 4.

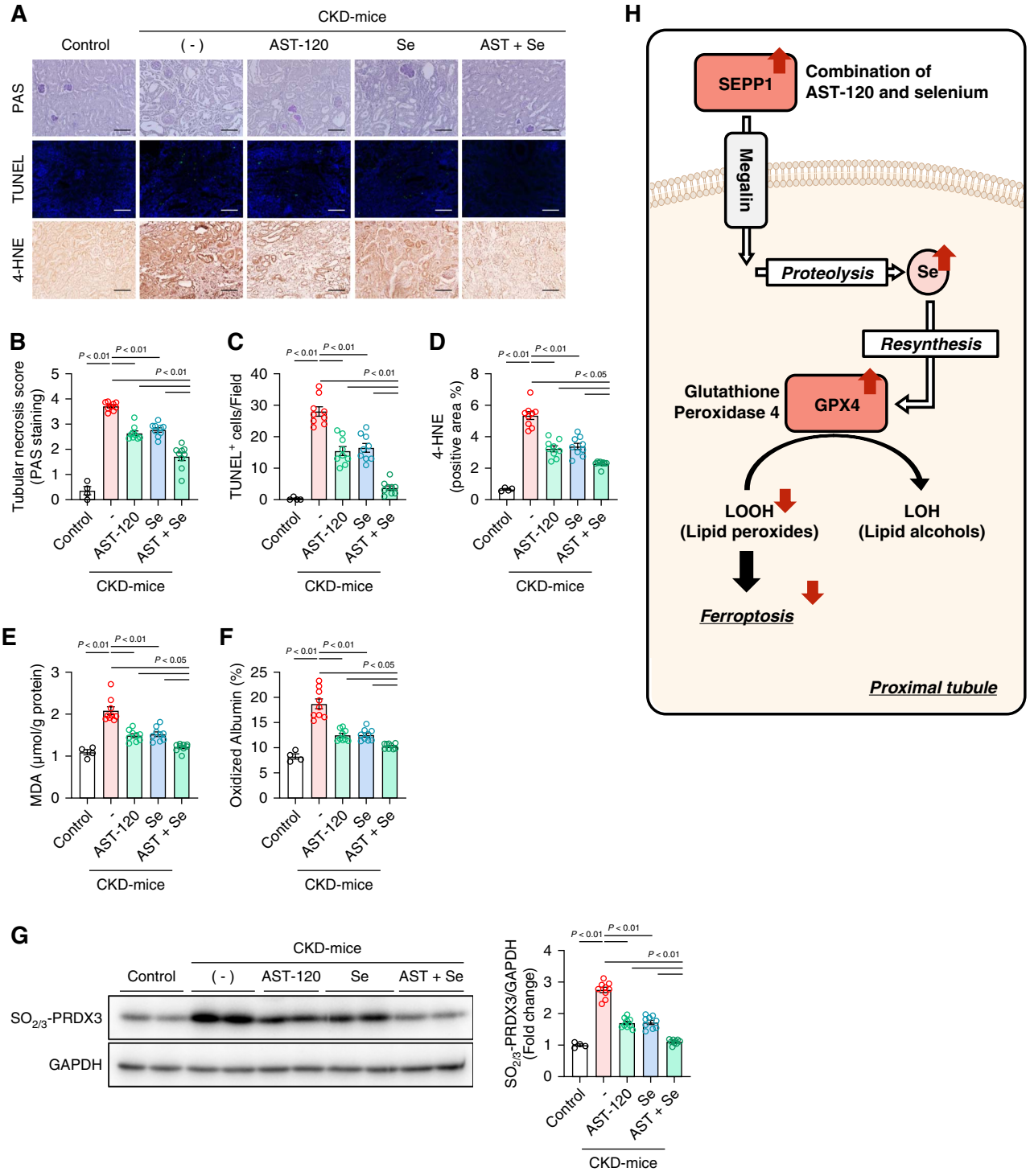

Figure 6. Renal protection by combination of AST-120 and Se supplementation in CKD mice. (A) Representative images of PAS staining (upper), TUNEL staining (middle), and immunostaining (lower) for 4-HNE. Scale bars=100 μm. (B) Tubular injury scoring. Quantification of (C) TUNEL-positive cells and (D) 4-HNE–positive area. (E) The MDA content in the kidney was determined using an MDA assay kit. (F) Oxidized albumin ratio was measured by ESI-TOF MS. (G) Hyperoxidized-PRDX3 ($SO_{2/3}$-PRDX3) protein expression in the kidney. (H) Schematic showing the molecular mechanism of renal protection by a combination of AST-120 and Se supplementation. Data are expressed as mean±SEM (n=4–9). 4-HNE, 4-hydroxynonenal; ESI-TOF MS, electrospray ionization time-of-flight mass spectrometry; MDA, malondialdehyde; PAS, periodic acid–Schiff; TUNEL, terminal deoxynucleotidyl transferase–mediated digoxigenin-deoxyuridine nick-end labeling.

restored by sodium selenite supplementation. Thus, exogenous supplementation of Se alone does not improve systemic Se deficiency. However, combination therapy with AST-120 resulted in a significant recovery of renal Se content (Figure 5F). These findings suggest restoring SEPP1 expression is crucial in CKD. Hence, the Se retention

capacity (*e.g.*, SEPP1 expression) of each patient should be assessed before administering Se supplementation. As shown in Supplemental Figure 4G, Se treatment alone significantly decreased plasma IS levels and improved kidney function. Although the reduction in plasma IS levels was smaller compared with AST-120 administration, other parameters, including plasma Se levels, SEPP1 expression, and protective effects on the kidney, are all comparable (Figures 5 and 6). As shown in Figure 5, F and G, Se treatment alone significantly increased renal Se content and GPX4 expression. This suggests that Se treatment also partially enables to supply Se to the kidney, which could exert its renal protective effects. These renoprotective effects by Se treatment could lead to reduced plasma IS levels (Supplemental Figure 4G). This suggests that Se treatment could partially exert its renoprotective effects through a different mechanism of action, independent of IS. Regarding the possible additive or synergistic effects of Se supplementation and AST-120, the combination index would be needed in the future. To clarify the contribution of Se deficiency on CKD progression, the experiment using mice with Se-deficient diet may be needed. In addition, the experiment in female mice to assess potential sex-specific differences would be needed in the future.

IS exhibited a dose-dependent suppressive effect on SEPP1 expression in HepG2 cells (Figure 3, C and D). Serum IS levels in uremic patients are typically approximately 100 μM but may be 1 mM.[39] These observations suggest that CKD patients with higher serum IS levels are more likely to exhibit Se deficiency because of reduced hepatic SEPP1 expression. Analysis of serum from patients on hemodialysis showed IS is associated with decreased serum SEPP1 levels and Se deficiency (Supplemental Figure 3, A and B). Therefore, serum IS levels could serve as a useful diagnostic marker for Se deficiency in CKD to guide decisions regarding Se supplementation therapy. Further clinical trials are needed to validate these findings.

Among seven albumin-binding uremic toxins (IS, *p*-cresyl sulfate, phenyl sulfate, hippuric acid, indole acetic acid, kynurenic acid, and carboxy-4-methyl-5-propyl-2-furanpropanoic), the strongest suppressive effect on SEPP1 expression was observed with IS (Figure 3, I and J). IS acts as a ligand for the AhR[40] and EGF receptor,[41] leading to the production of ROS. Activation of NADPH oxidase is involved in each ROS production pathway.[40,42] The decrease in SEPP1 expression induced by IS was significantly suppressed by inhibitors of AhR (CH-223191) and NADPH oxidase (diphenylene iodonium; Figure 4A). In addition, among the seven uremic toxins tested in HepG2 cells, IS showed the greatest increase in ROS production (Figure 4C). When hydrogen peroxide, a ROS inducer, was added to HepG2 cells, SEPP1 expression decreased, and this effect was suppressed in the presence of AsA (Figure 4B). Thus, the increase in ROS production by IS is involved in the suppression of SEPP1 expression. To validate the mechanism that connects renal ferroptosis and IS to Se deprivation, it would be desirable to evaluate the *in vivo* effect of OATP/AhR/NADPH oxidase pathway inhibitor in the future.

We identified involvement of the AMPK/PGC-1α pathway and miR-34a/HNF4α pathway in IS-induced ROS production (Figure 4, D–H). Previous studies reported that IS induces dephosphorylation of AMPK,[30,43,44] but this is the first to demonstrate a relationship with ROS production. ROS increases miR-34a expression through the kelch-like ECH-associated protein 1/Nuclear factor erythroid 2-related factor 2 pathway.[45] Intriguingly, miR-34a is associated with kidney aging by suppressing mitochondrial antioxidant enzymes, such as superoxide dismutase 2 and Txnrd2, as well as with kidney fibrosis through the suppression of Klotho expression in renal tubules.[46,47] These findings suggest that, in addition to its effect on SEPP1 expression, miR-34a may also be involved in the progression of CKD.

The redox balance in renal tubules is closely regulated by the Se-containing protein GPX4. Indeed, GPX4 knockout mice develop AKI associated with tubular ferroptosis.[35] Several studies have aimed to elucidate mechanisms that maintain GPX4 expression in renal tubules and suppress ferroptosis.[48–50] In this study, we demonstrated that the reduction in renal Se content in CKD mice contributes to decreased GPX4 expression (Figure 5, F–H). We also showed that combination therapy with AST-120 and sodium selenite restored Se supply and GPX4 expression in the kidneys, leading to kidney protection by suppression of ferroptosis (Figure 6). A therapeutic approach aimed at preventing Se reduction in CKD, thereby restoring GPX4 expression and inhibiting ferroptosis in renal tubules, has not previously been reported. Spherical adsorbent carbon, represented by AST-120, is marketed as a drug to suppress CKD progression in several countries (Japan [since 1991], South Korea [since 2004], Taiwan [since 2007], and the Philippines [since 2010]).[51] In addition, sodium selenite injection is approved as a treatment of Se deficiency[52] and its safety in patients on hemodialysis confirmed.[53] Therefore, there would be few barriers to the clinical application of this combination therapy. This study provides foundational data for the potential application of a combined therapy comprising spherical adsorbent carbon and injection of sodium selenite for patients with CKD.

Disclosures

Disclosure forms, as provided by each author, are available with the online version of the article at http://links.lww.com/KN9/B75.

Funding

H. Watanabe: Japan Society for the Promotion of Science (KAKENHI JP23K28431 and JP20H03406), T. Nakano: Japan Society for the Promotion of Science (JST SPRING JPMJSP2127).

Author Contributions

Conceptualization: Takehiro Nakano, Hiroshi Watanabe, Kohei Yasuno, Takuma Yoshitake.
Data curation: Takehiro Nakano.
Formal analysis: Takehiro Nakano.
Investigation: Yutaka Kitazato, Takehiro Nakano, Takumu Ogawa, Yuhi Shintani, Kai Tokumaru.
Methodology: Takehiro Nakano.
Supervision: Hitoshi Maeda, Toru Maruyama, Kazutaka Matsushita, Motoko Tanaka, Hiroshi Watanabe.
Visualization: Takehiro Nakano.
Writing – original draft: Takehiro Nakano.
Writing – review & editing: Hiroshi Watanabe.

Data Sharing Statement

Partial restrictions to the data and/or materials apply. Data will be available upon reasonable request to the corresponding author.

Supplemental Material

This article contains the following supplemental material online at http://links.lww.com/KN9/B76.

Supplemental Methods

Supplemental Table 1. Plasma biochemical parameters in CKD mice. BUN and serum creatinine for control mice and 0.2% adenine-containing diet–fed mice without/with AST-120 treatment.

Supplemental Table 2. Plasma trace element parameters in CKD mice. Se, Zn, and Fe for control mice and 0.2% adenine-containing diet–fed mice without/with AST-120 treatment.

Supplemental Table 3. List of antibodies for Western blotting (upper table), RNA primers (middle table), and stem-loop miRNA primers (lower table) for quantitative RT-PCR.

Supplemental Figure 1. Effect of IS on liver SEPP1 expression and Se kinetic studies in the 5/6Nx mouse model.

Supplemental Figure 2. Molecular mechanism of IS-induced SEPP1 suppression.

Supplemental Figure 3. Serum Se level in patients on hemodialysis.

Supplemental Figure 4. Therapeutic intervention targeting the IS/SEPP1 pathway in CKD mice.

Supplemental References

References

1. Reimer KC, Nadal J, Meiselbach H, et al.; GCKD study investigators. Association of mineral and bone biomarkers with adverse cardiovascular outcomes and mortality in the German Chronic Kidney Disease (GCKD) cohort. *Bone Res.* 2023;11(1):52. doi:10.1038/s41413-023-00291-8
2. Edmonston D, Wolf M. FGF23 at the crossroads of phosphate, iron economy and erythropoiesis. *Nat Rev Nephrol.* 2020;16(1):7–19. doi:10.1038/s41581-019-0189-5
3. Tonelli M, Wiebe N, Bello A, et al.; Alberta Kidney Disease Network. Concentrations of trace elements and clinical outcomes in hemodialysis patients: a prospective cohort study. *Clin J Am Soc Nephrol.* 2018;13(6):907–915. doi:10.2215/CJN.11451017
4. Yasukawa M, Arai S, Nagura M, et al. Selenium associates with response to erythropoiesis-stimulating agents in hemodialysis patients. *Kidney Int Rep.* 2022;7(7):1565–1574. doi:10.1016/j.ekir.2022.04.009
5. Zhu D, Zhong Q, Lin T, Song T. Higher serum selenium concentration is associated with lower risk of all-cause and cardiovascular mortality among individuals with chronic kidney disease: a population-based cohort study of NHANES. *Front Nutr.* 2023;10:1127188. doi:10.3389/fnut.2023.1127188
6. Joo YS, Kim HW, Lee S, et al. Dietary zinc intake and incident chronic kidney disease. *Clin Nutr.* 2021;40(3):1039–1045. doi:10.1016/j.clnu.2020.07.005
7. Nakatani S, Mori K, Shoji T, Emoto M. Association of zinc deficiency with development of CVD events in patients with CKD. *Nutrients.* 2021;13(5):1680. doi:10.3390/nu13051680
8. Fujishima Y, Ohsawa M, Itai K, et al. Serum selenium levels are inversely associated with death risk among hemodialysis patients. *Nephrol Dial Transplant.* 2011;26(10):3331–3338. doi:10.1093/ndt/gfq859
9. Maruyama Y, Nakashima A, Fukui A, Yokoo T. Zinc deficiency: its prevalence and relationship to renal function in Japan. *Clin Exp Nephrol.* 2021;25(7):771–778. doi:10.1007/s10157-021-02046-3
10. Kimmel PL, Watkins DW, Teller EB, Khanna R, Dosa S, Phillips TM. Zinc balance in combined zinc deficiency and uremia. *Kidney Int.* 1988;33(6):1091–1099. doi:10.1038/ki.1988.116
11. Tokuyama A, Kanda E, Itano S, et al. Effect of zinc deficiency on chronic kidney disease progression and effect modification by hypoalbuminemia. *PLoS One.* 2021;16(5):e0251554. doi:10.1371/journal.pone.0251554
12. Damianaki K, Lourenco JM, Braconnier P, et al. Renal handling of zinc in chronic kidney disease patients and the role of circulating zinc levels in renal function decline. *Nephrol Dial Transplant.* 2020;35(7):1163–1170. doi:10.1093/ndt/gfz065
13. Oka T, Hamano T, Sakaguchi Y, et al. Proteinuria-associated renal magnesium wasting leads to hypomagnesemia: a common electrolyte abnormality in chronic kidney disease. *Nephrol Dial Transplant.* 2019;34(7):1154–1162. doi:10.1093/ndt/gfy119
14. Bushinsky DA, Spiegel DM, Yuan J, Warren S, Fogli J, Pergola PE. Effects of the potassium-binding polymer patiromer on markers of mineral metabolism. *Clin J Am Soc Nephrol.* 2019;14(1):103–110. doi:10.2215/CJN.04500418
15. Hamano H, Ikeda Y, Watanabe H, et al. The uremic toxin indoxyl sulfate interferes with iron metabolism by regulating hepcidin in chronic kidney disease. *Nephrol Dial Transplant.* 2018;33(4):586–597. doi:10.1093/ndt/gfx252
16. Watanabe K, Tominari T, Hirata M, et al. Indoxyl sulfate, a uremic toxin in chronic kidney disease, suppresses both bone formation and bone resorption. *FEBS Open Bio.* 2017;7(8):1178–1185. doi:10.1002/2211-5463.12258
17. Charni-Natan M, Goldstein I. Protocol for primary mouse hepatocyte isolation. *STAR Protoc.* 2020;1(2):100086. doi:10.1016/j.xpro.2020.100086
18. Saito Y. Selenium transport mechanism via selenoprotein P-its physiological role and related diseases. *Front Nutr.* 2021;8:685517. doi:10.3389/fnut.2021.685517
19. Jujic A, Molvin J, Schomburg L, et al. Selenoprotein P deficiency is associated with higher risk of incident heart failure. *Free Radic Biol Med.* 2023;207:11–16. doi:10.1016/j.freeradbiomed.2023.07.007
20. Schweizer U, Wirth EK, Klopstock T, et al. Seizures, ataxia and parvalbumin-expressing interneurons respond to selenium supply in Selenop-deficient mice. *Redox Biol.* 2022;57:102490. doi:10.1016/j.redox.2022.102490
21. Thomson CD, Burton CE, Robinson MF. On supplementing the selenium intake of New Zealanders. 1. Short experiments with large doses of selenite or selenomethionine. *Br J Nutr.* 1978;39(3):579–587. doi:10.1079/bjn19780073
22. Lobinski R, Edmonds JS, Suzuki KT, Uden PC. Species-selective determination of selenium compounds in biological materials (Technical Report). *Pure Appl Chem.* 2000;72(3):447–461. doi:10.1351/pac200072030447
23. Olson GE, Winfrey VP, Hill KE, Burk RF. Megalin mediates selenoprotein P uptake by kidney proximal tubule epithelial cells. *J Biol Chem.* 2008;283(11):6854–6860. doi:10.1074/jbc.M709945200
24. Chiu-Ugalde J, Theilig F, Behrends T, et al. Mutation of megalin leads to urinary loss of selenoprotein P and selenium deficiency in serum, liver, kidneys and brain. *Biochem J.* 2010;431(1):103–111. doi:10.1042/BJ20100779
25. Schwarz M, Meyer CE, Löser A, et al. Excessive copper impairs intrahepatocyte trafficking and secretion of selenoprotein P. *Nat Commun.* 2023;14(1):3479. doi:10.1038/s41467-023-39245-3
26. Nakano T, Katsuki S, Chen M, et al. Uremic toxin indoxyl sulfate promotes proinflammatory macrophage activation via the interplay of OATP2B1 and Dll4-Notch signaling. *Circulation.* 2019;139(1):78–96. doi:10.1161/CIRCULATIONAHA.118.034588
27. Tajima-Shirasaki N, IshiiK-A, Takayama H, et al. Eicosapentaenoic acid down-regulates expression of the selenoprotein P gene by inhibiting SREBP-1c protein independently of the AMP-activated protein kinase pathway in H4IIEC3 hepatocytes. *J Biol Chem.* 2017;292(26):10791–10800. doi:10.1074/jbc.M116.747006
28. Speckmann B, Walter PL, Alili L, et al. Selenoprotein P expression is controlled through interaction of the coactivator PGC-1alpha with FoxO1a and hepatocyte nuclear factor 4alpha transcription factors. *Hepatology.* 2008;48(6):1998–2006. doi:10.1002/hep.22526
29. Enoki Y, Watanabe H, Arake R, et al. Potential therapeutic interventions for chronic kidney disease-associated sarcopenia

via indoxyl sulfate-induced mitochondrial dysfunction. *J Cachexia Sarcopenia Muscle.* 2017;8(5):735–747. doi:10.1002/jcsm.12202
30. Yang K, Xu X, Nie L, et al. Indoxyl sulfate induces oxidative stress and hypertrophy in cardiomyocytes by inhibiting the AMPK/UCP2 signaling pathway. *Toxicol Lett.* 2015;234(2):110–119. doi:10.1016/j.toxlet.2015.01.021
31. Li X, Lu Z, Zhou F, et al. Indoxyl sulfate promotes the atherosclerosis through up-regulating the miR-34a expression in endothelial cells and vascular smooth muscle cells in vitro. *Vascul Pharmacol.* 2020;131(106763):106763. doi:10.1016/j.vph.2020.106763
32. Xu Y, Zalzala M, Xu J, Li Y, Yin L, Zhang Y. A metabolic stress-inducible miR-34a-HNF4α pathway regulates lipid and lipoprotein metabolism. *Nat Commun.* 2015;6(1):7466. doi:10.1038/ncomms8466
33. Oo SM, Misu H, Saito Y, et al. Serum selenoprotein P, but not selenium, predicts future hyperglycemia in a general Japanese population. *Sci Rep.* 2018;8(1):16727. doi:10.1038/s41598-018-35067-2
34. Mishima E, Conrad M. Nutritional and metabolic control of ferroptosis. *Annu Rev Nutr.* 2022;42(1):275–309. doi:10.1146/annurev-nutr-062320-114541
35. Friedmann Angeli JP, Schneider M, Proneth B, et al. Inactivation of the ferroptosis regulator Gpx4 triggers acute renal failure in mice. *Nat Cell Biol.* 2014;16(12):1180–1191. doi:10.1038/ncb3064
36. KungW-J, ShihC-T, LeeC-H, LinC-C. The divalent elements changes in early stages of chronic kidney disease. *Biol Trace Elem Res.* 2018;185(1):30–35. doi:10.1007/s12011-017-1228-3
37. Lin T, Tao J, Chen Y, et al. Selenium deficiency leads to changes in renal fibrosis marker proteins and Wnt/β-catenin signaling pathway components. *Biol Trace Elem Res.* 2022;200(3):1127–1139. doi:10.1007/s12011-021-02730-1
38. Zachara BA, Trafikowska U, Adamowicz A, Nartowicz E, Manitius J. Selenium, glutathione peroxidases, and some other antioxidant parameters in blood of patients with chronic renal failure. *J Trace Elem Med Biol.* 2001;15(2-3):161–166. doi:10.1016/S0946-672X(01)80061-4
39. Vanholder R, Schepers E, Pletinck A, Nagler EV, Glorieux G. The uremic toxicity of indoxyl sulfate and p-cresyl sulfate: a systematic review. *J Am Soc Nephrol.* 2014;25(9):1897–1907. doi:10.1681/ASN.2013101062
40. Nakagawa K, Itoya M, Takemoto N, et al. Indoxyl sulfate induces ROS production via the aryl hydrocarbon receptor-NADPH oxidase pathway and inactivates NO in vascular tissues. *Life Sci.* 2021;265:118807. doi:10.1016/j.lfs.2020.118807
41. Jansen J, Jansen K, Neven E, et al. Remote sensing and signaling in kidney proximal tubules stimulates gut microbiome-derived organic anion secretion. *Proc Natl Acad Sci U S A.* 2019;116(32):16105–16110. doi:10.1073/pnas.1821809116
42. Poursaitidis I, Wang X, Crighton T, et al. Oncogene-Selective sensitivity to synchronous cell death following modulation of the amino acid nutrient cystine. *Cell Rep.* 2017;18(11):2547–2556. doi:10.1016/j.celrep.2017.02.054
43. Chen C, Wu L, Xie C, Zhao X, Mao H, Xing C. The role of AMP-activated protein kinase α1-mediated endoplasmic reticulum stress in alleviating the toxic effect of uremic toxin indoxyl sulfate on vascular endothelial cells by Klotho. *J Appl Toxicol.* 2021;41(9):1446–1455. doi:10.1002/jat.4135
44. Kikuchi H, Sasaki E, Nomura N, et al. Failure to sense energy depletion may be a novel therapeutic target in chronic kidney disease. *Kidney Int.* 2019;95(1):123–137. doi:10.1016/j.kint.2018.08.030
45. Liu C, Rokavec M, Huang Z, Hermeking H. Curcumin activates a ROS/KEAP1/NRF2/miR-34a/b/c cascade to suppress colorectal cancer metastasis. *Cell Death Differ.* 2023;30(7):1771–1785. doi:10.1038/s41418-023-01178-1
46. BaiX-Y, Ma Y, Ding R, Fu B, Shi S, ChenX-M. miR-335 and miR-34a Promote renal senescence by suppressing mitochondrial antioxidative enzymes. *J Am Soc Nephrol.* 2011;22(7):1252–1261. doi:10.1681/ASN.2010040367
47. Liu Y, Bi X, Xiong J, et al. MicroRNA-34a promotes renal fibrosis by downregulation of Klotho in tubular epithelial cells. *Mol Ther.* 2019;27(5):1051–1065. doi:10.1016/j.ymthe.2019.02.009
48. ChuL-K, Cao X, Wan L, et al. Autophagy of OTUD5 destabilizes GPX4 to confer ferroptosis-dependent kidney injury. *Nat Commun.* 2023;14(1):8393. doi:10.1038/s41467-023-44228-5
49. Sun X, Huang N, Li P, et al. TRIM21 ubiquitylates GPX4 and promotes ferroptosis to aggravate ischemia/reperfusion-induced acute kidney injury. *Life Sci.* 2023;321:121608. doi:10.1016/j.lfs.2023.121608
50. Deng Z, Wang Y, Liu J, et al. WBP2 restrains the lysosomal degradation of GPX4 to inhibit ferroptosis in cisplatin-induced acute kidney injury. *Redox Biol.* 2023;65:102826. doi:10.1016/j.redox.2023.102826
51. Schulman G, Berl T, Beck GJ, et al. Randomized placebo-controlled EPPIC trials of AST-120 in CKD. *J Am Soc Nephrol.* 2015;26(7):1732–1746. doi:10.1681/ASN.2014010042
52. Abdulah R, Katsuya Y, Kobayashi K, et al. Effect of sodium selenite supplementation on the levels of prostacyclin I(2) and thromboxane A(2) in human. *Thromb Res.* 2007;119(3):305–310. doi:10.1016/j.thromres.2006.02.005
53. Richard MJ, Ducros V, Forêt M, et al. Reversal of selenium and zinc deficiencies in chronic hemodialysis patients by intravenous sodium selenite and zinc gluconate supplementation. Time-course of glutathione peroxidase repletion and lipid peroxidation decrease. *Biol Trace Elem Res.* 1993;39(2-3):149–159. doi:10.1007/bf02783185

AFFILIATIONS

[1]Department of Biopharmaceutics, Graduate School of Pharmaceutical Sciences, Kumamoto University, Kumamoto, Japan
[2]Department of Clinical Pharmacy and Therapeutics, Graduate School of Pharmaceutical Sciences, Kumamoto University, Kumamoto, Japan
[3]Department of Nephrology, Akebono Clinic, Kumamoto, Japan